Saint Martin's University

Simulating a Piezoelectric-Haptic MEMS Actuator in Low-Frequency Vibration

By Alexander Benson and Seth Carl

Table of Contents

Abstract

Haptics are a popular method for providing supplemental feedback. When experiencing ambiguous feedback, users can rely on haptics as another modality to compensate for the presence of noise. Designers frequently rely on haptics for the quick response touch and proprioception can provoke from the user, such as the Tactile Awareness System relied on by combat helicopter pilots. Tactile feedback does not suffer from some of the limitations of other modalities; haptic actuators are being integrated into steering wheels to provide lane departure warnings for distracted drivers. As such, the development and qualification of new haptic feedback methods represents foundational work for future engineers and user experience designers.

The authors explored the idea of a haptic mouse exploiting a documented phenomenon in which tangential loads to a user's finger are aliased with positional cues. Feedback could not be restricted to a narrow range of vibrations and high-resolution positional control would be critical. Piezoelectric actuators were ideal because they have a broad range of actuation modes; positional actuation is possible, and a continuous range of vibrations is supported into ultrasonic frequencies. The broad vibration range stands in contrast to linear resonance actuators, which have a narrow band of operating frequencies. A flextension-style microelectromechanical system (MEMS) was designed to increase the range of actuation possible with the piezoelectrics preferred by a factor of nearly 10. The flextensional system converted the piezoelectric actuator into a two-degree-of-freedom (DOF) system, with the piezoactuator serving as a cyclic force. The actuator was intended to provide a wide range of feedback, the primary modality being the aliased positional cues with vibration as a secondary feedback mode. For simplicity, a single axis of the complete system was studied and designed.

Simulations of a piezoelectric actuator vibrating with and without a human finger resting on the actuator were studied. The actuator resembles a two DOF system without a finger. With a finger, the actuator becomes a three DOF system. All systems were simulated using MATLAB's ODE45 solver. Closed-form solutions of single DOF systems are easily calculated; however, the ODE45 solver was used to simulate the single DOF systems for the sake of consistency and to prevent the introduction of confounding variables.

The quality of a single-degree-of-freedom reduction depended on whether the user's finger was considered. Without a finger, no significant deviations in the system's behavior were found; the equivalent spring, mass, and damper coefficients match those calculated by standard reduction methods without complication. The addition of a finger complicated the simulation. The frequency behavior of the single-degree-of-freedom system dropped an order of magnitude below the frequencies of the multi-degree-of-freedom system. This drop resulted in discrepancies between the simulated behavior of the multi-degree-of-freedom and its single-degree-of-freedom equivalent.

Introduction and Project Significance

Dialectica is working on an information management system used to deconstruct highly organized information structures and process them into a manageable format [1]. This system relies on creating a spatial structure that humans then navigate, the idea being that spatially located concepts are better retained [2]. Human-OS interaction suffers from a disconnect in that the interactions exist strictly in auditory and visual modes. Touch and proprioception, the foundations of haptic design, are essential in creating a sense of space beyond what can be immediately seen and heard. Touch can convey a physicality that vision and audition cannot [3] and is an essential component in processing noisy cues from other senses [4].

In developing a multi-axis haptic mouse, focus on a single actuator axis took priority for the sake of system refinement and development. The single-axis system can be seen as actuator system 1 in Figure 1. Characterizing the behavior of a haptic mouse is an essential step in improving the quality of human-machine interfaces. It was thought that the exploitation of the aliasing of position cues with tangential load to the finger would allow for redundant locational cues within the Dialectic space[1], [2], [5]. The solution that met project needs in the near term exploited the combination of piezo actuators and microelectromechanical systems (MEMS).

The vibration behavior of a haptic mouse emerged as a salient point in the design process. The system was initially intended to closely alias the mouse's motion with the oscillations of the haptic device, only requiring support for low-frequency vibrations. With consideration, higher frequencies might represent additional feedback modalities and arbitrary forcing conditions could further exploit the aliasing of force-position cues. For these reasons, determining whether the system with applied finger force and without it could be reduced to a single-degree-of-freedom was a priority.

Operating Principle

The displacement possible in small-scale actuators is limited[6]. For that reason, micromotion amplification methods[7] would be used to extend the displacement range to the low end of the typical detection range for bump detection. An exploded-view can be seen in Figure 1. The haptic package was to be as small as possible, minimizing the amount of space occupied by the device. For this reason, one actuator would amplify motion in line with the actuator, upper left, while the other actuator would amplify motion orthogonal to the actuator, upper right. The final axis would be mounted to a pin and actuate vertically, see the final assembly in Figure 2. There was a high likelihood that the carriages and pin necessary to operate this system would behave like spring-damper systems. To ensure consistent operation, it was deemed necessary to verify that the system's resonance modes would not be activated mid-use.

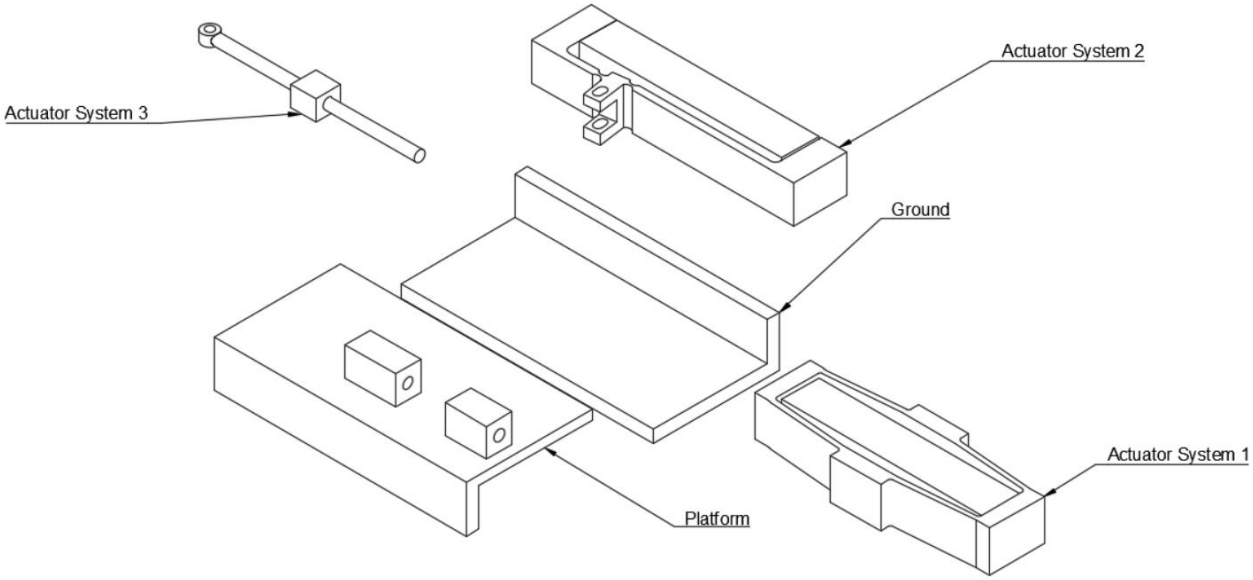

Figure 1: An exploded view of the system

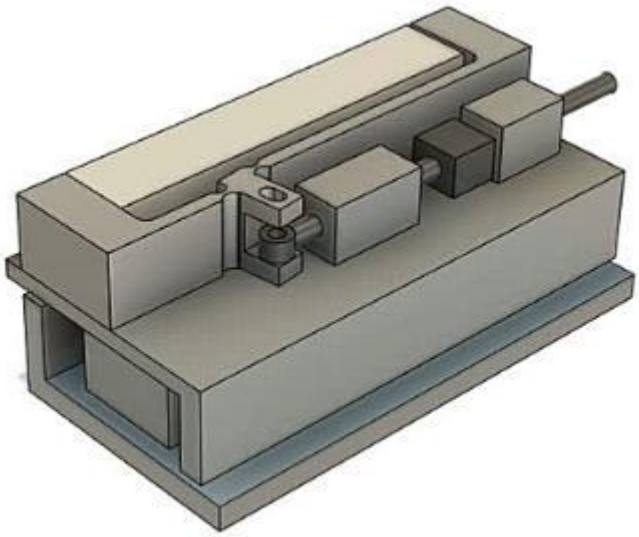

Figure 2: The system as assembled

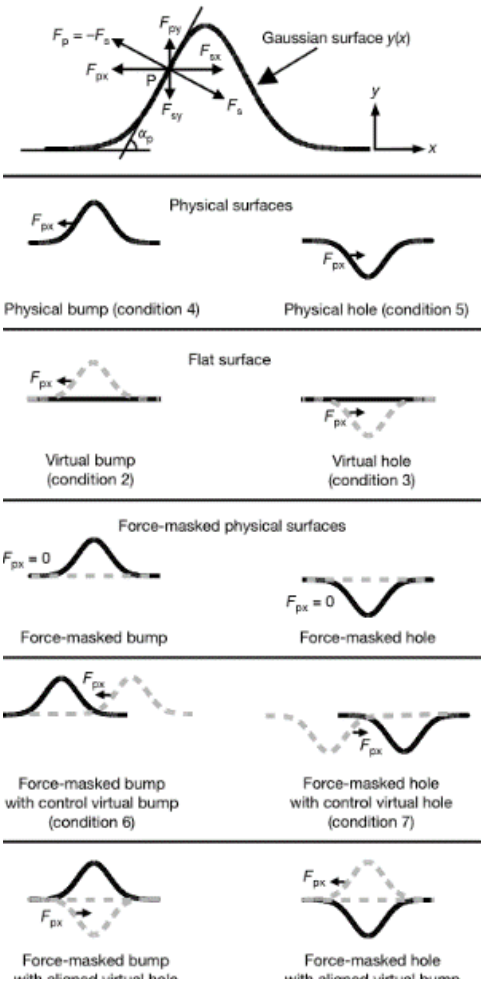

Figure 3: Methods for generating artificial bumps and suppressing actual surface features[5]

Literature Review and State of the Art

Tests have suggested haptics is a helpful cue, assisting humans with correcting and removing the noise from a given cue or input[4]. Haptic feedback can take many forms, from an electro-tactile display for the blind that converts an image into an array of sensations felt by the tongue to more familiar braille-like systems formed by pins. Many applications of haptic displays and feedback are familiar in one form or another:

- Vehicles are being outfitted with vibratory feedback, alerting drivers to lane departure.
- The Tactile Situation Awareness System improves helicopter pilot confidence and performance by providing non-visual feedback to the user. This supplementary interface is effective even in low-visibility conditions[3].

Many portable haptic devices do not have the geometry necessary for conventional force feedback. In these scenarios, it is possible to create the illusion of a bump or hole on a flat surface. This illusion is achieved by generating a tangential load to the finger, which will be perceived as a position cue and a force load. It appears that the position-force cue confusion is a function of the brain favoring the force cues statistically consistent with a bump and ignoring contradictory position cues of lower quality[8]. It is possible to mask holes and bumps with a sufficiently sensitive system, see Figure 3[5], [8].

Similar devices to the design studied have been explored. The small range of motion available to a piezo actuator means that these devices have, historically, been relatively large[9], [10]. Microelectromechanical systems are an emerging field, addressing the limitations of piezo actuators by amplifying or modifying the range of motion available to actuators. For the flextensional system selected, the amplification is approximately the cotangent of θ, θ being the angle formed by the moving arm and the horizontal axis. Flextensional systems have limitations in that the direction of piezo actuation is orthogonal to the motion of the actuator[7].

Quantification of the spring-mass-damper behavior of a finger was critical to the system studied. Previous research indicates that the fingertip behaves as an elastic system below ~100hz and a viscously damped system beyond. The parameters tested varied depending on the test subject. The elasticity was found to have a range of $0.6 - 2.0\ {}^{\mathrm{kN}}/_{\mathrm{m}}$, the damping was $0.75 - 2.38\ {}^{N\ -\ s}/_{m}$, and effective masses ranged from 110-230mg[11].

Simplification to a single axis system:

The system presented uses three piezoelectric actuators to move a platform where the finger will rest. This platform can move in all three dimensions to allow for diverse haptic feedback to the finger. When reduced to a paper model, the mechanical system indicates four degrees of freedom. Simplification to a single-degree-of-freedom requires the reduction to one axis of movement. The haptic development process requires that the team (Dialectica's haptic developers) characterize the degree to which a piezoactuator can activate the Hayward and Robles Phenomenon. For these testing purposes, a single-dimensional actuator has been developed[1]. One node is left connected to the platform and ground by removing two of the three piezoelectric actuators. This actuator acts as the x-dimension. Once this is completed, the system operates in a single dimension and contains two degrees of freedom. Their relationship can be shown in a two-degrees-of-freedom equation of motion.

Simplification Method – A complicated Single-degree-of-freedom System to a Spring-Mass-Damper System

For manufacturing purposes, actuator system 1 has been redesigned, see Figure 4, since the rendering of the entire haptic system in Figure 1. The visible gap at one end exists to support the manufacturing tolerances of the piezoactuator ($\pm 0.5\text{mm}$ on the longest axis) and would be filled with adhesive to eliminate the gap as needed. The redesigned flextension system can be fabricated from sheet metal (1095 spring steel, for example). As designed, the system is an actuation amplifier typical of many microelectromechanical systems (MEMS)[7].

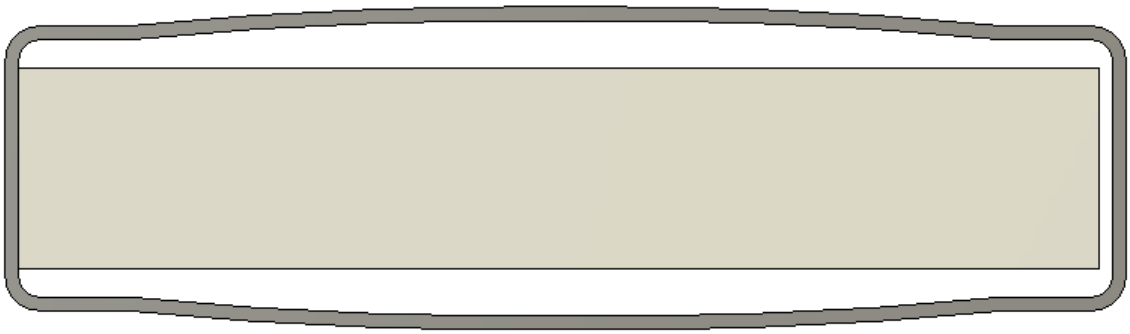

Figure 4: The redesigned actuator system 1

[1] Rendered as “Actuator System 1” in Figure 4

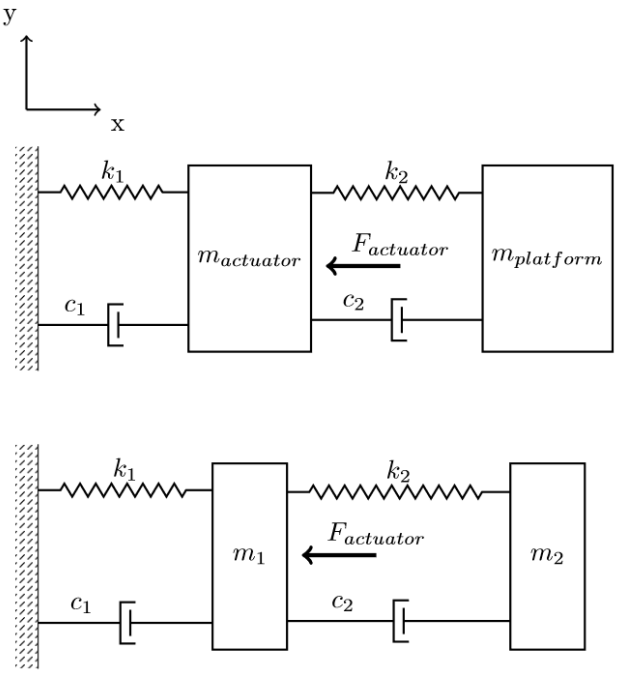

Figure 5: The built-out system for actuator 1, 2 DOF

As designed, the piezoactuator would extend $42\mu m$ with a motion amplification factor of 10. The result of this motion is that the actuator face attached to "ground" would remain stationary, the piezoactuator (labeled as m_1 in Figure 5) would move $210\mu m$, and the rest of the test system[2] (labeled as m_2) would move $420\mu m$. For this reason, any motion of the actuator would be treated as equivalent to half the motion of the test system.

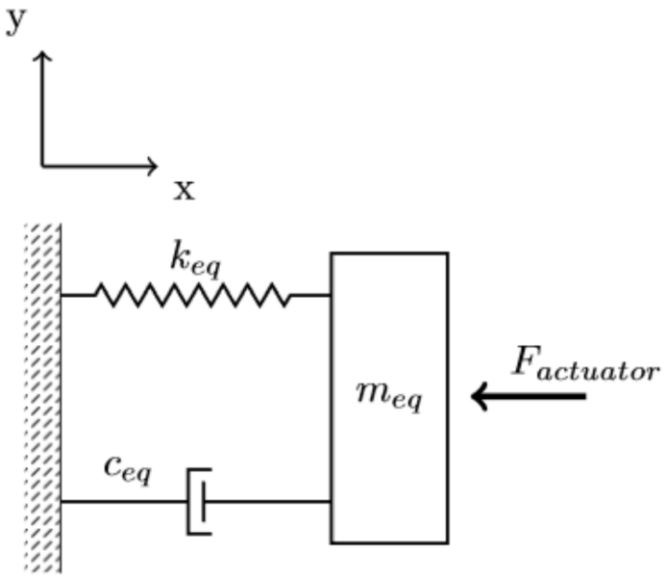

Figure 6: The single DOF simplified system

[2] Assumed to be a platform and user's finger for the purposes of this test

Actuator Force

Force equivalence is shown in the simplified system as the forces applied by the actuator to the equivalent mass, see Figure 6. The force applied by the actuator is placed opposite to the forces applied by $\mathrm{k_{eq}}$ and $\mathrm{c_{eq}}$. The force applied by the actuator is an alternating force described as $\mathrm{F_0 cos(\omega t)}$. The value of $\mathrm{F_0}$ would be subject to change depending on the context of user interaction. ANSYS simulation suggests that the maximum displacement of the system would exert $85.68\mathrm{N}$. As a result, $\mathrm{F_0} = 85\mathrm{N}$ would be the assumed force in mathematical simulations.

The user and the interface would dictate the wavelengths generated by the actuator. A user may pass over a bump multiple times in rapid succession, resulting in a vibration response in normal use. It is unlikely that the user would be capable of exceeding 20hz, given that it would require the user to move their hand back and forth at 20 times a second. However, future applications may rely on vibration as a feedback modality. For this reason higher frequencies were entertained.

Equations of Motion - System without Finger – Two-DOF

The equation of motion for the system can be found using the single-axis system shown in Figure 5. In this context, $\mathrm{x_1}$ is the net displacement of the spring to the left of mass m, $\mathrm{x_2}$ is the displacement of the spring to the right of mass m. This is, arguably, an unnecessary distinction given that $2\mathrm{x_1} = \mathrm{x_2}$ if the system performs as designed.

$$\begin{bmatrix} m_1 & 0 \\ 0 & m_2 \end{bmatrix} \begin{Bmatrix} \ddot{x}_1 \\ \ddot{x}_2 \end{Bmatrix} + \begin{bmatrix} c_1 + c_2 & -c_2 \\ -c_2 & c_2 \end{bmatrix} \begin{Bmatrix} \dot{x}_1 \\ \dot{x}_2 \end{Bmatrix} + \begin{bmatrix} k_1 + k_2 & -k_2 \\ -k_2 & k_2 \end{bmatrix} \begin{Bmatrix} \mathrm{x_1} \\ x_2 \end{Bmatrix} = \begin{Bmatrix} F_{actuator} \\ 0 \end{Bmatrix} \quad (1)$$

Spring Equivalence

The curvature of the flextensional system complicated hand calculations. For this reason, the flextension system was simulated in ANSYS, see Figure 7. This simulation suggests that the net spring equivalent for the system is approximately 204N/mm. Given the system's symmetry, the spring constants are assumed to be equivalent. Given this assumption, a 204N/mm equivalence corresponds to individual constants, $\mathrm{k_1}$ and k_2, of 408N/mm, see Equation 2:

$$k_{eq} = \frac{1}{\frac{1}{k_1} + \frac{1}{k_2}} \Rightarrow \qquad \mathrm{k_{eq}} = \frac{1}{\frac{1}{\mathrm{k}} + \frac{1}{k}} = \frac{k}{2} \quad (2)$$

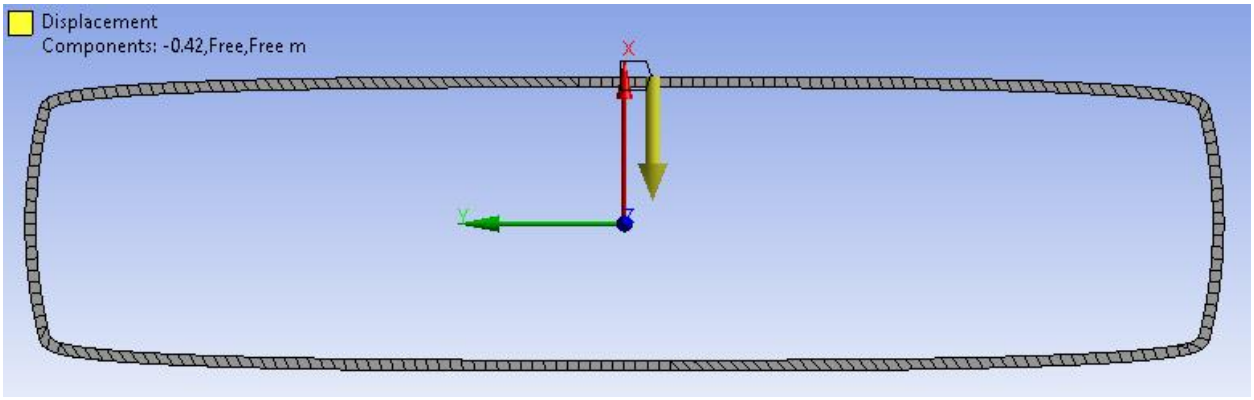

Figure 7: The prescribed displacement in the FEA analysis of the actuator system

Dampening Equivalence

The damping coefficients were derived using an assumption of symmetry similar to the spring derivation. From Figure 5, it was assumed that the dampers are in series; therefore, the dampening equivalent can be summarized by Equation 3:

$$c_{eq} = \frac{1}{\frac{1}{c_1}+\frac{1}{c_2}} \Rightarrow \qquad \mathrm{c_{eq}} = \frac{1}{\frac{1}{\mathrm{c}}+\frac{1}{\mathrm{c}}} = \frac{\mathrm{c}}{2} \tag{3}$$

Using ANSYS, a modal analysis of the flextension system found the system to have a damped frequency of 511.6Hz in the desired bending/flexing mode, as shown in Figure 8.

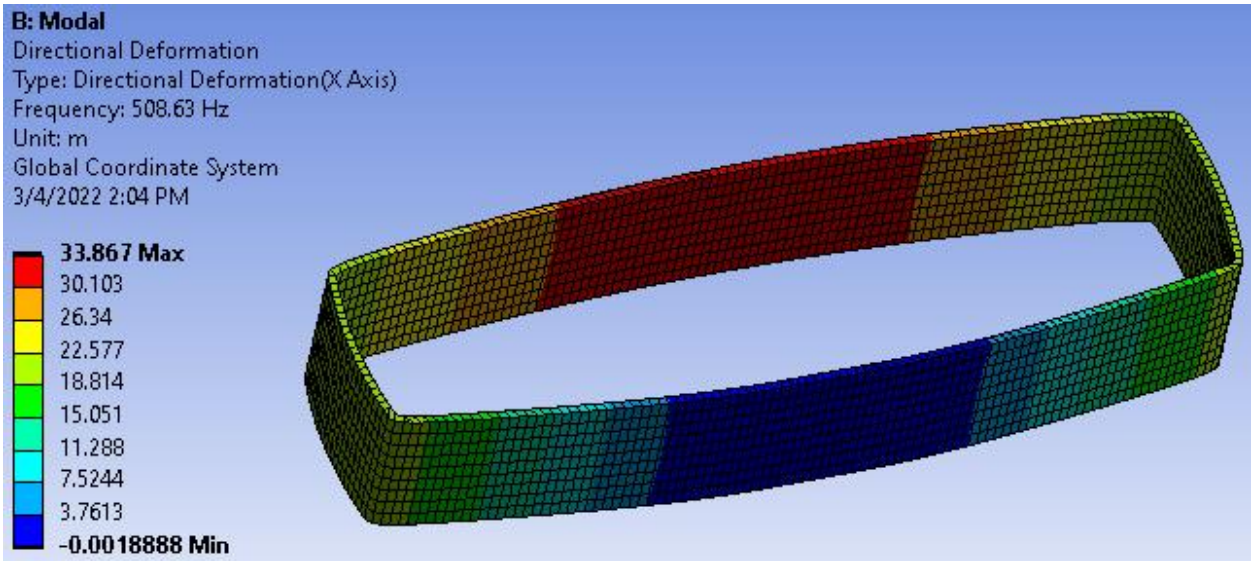

Figure 8: The modal analysis of the flextension system

Using the damped frequency found in ANSYS, the damped ratio can be found using the following equation:

$$\omega_d = \omega_n\sqrt{1-\zeta^2} \qquad \Rightarrow \qquad \zeta = \sqrt{1-\left(\frac{\omega_d}{\omega_n}\right)^2} \tag{4}$$

where the natural frequency can be defined as the square root of the equivalent spring constant divided by the equivalent mass constant as shown:

$$\omega_n = \sqrt{k/m} = \sqrt{k_{eq}/m_{eq}} \tag{5}$$

Through equation 4, the damping ratio was found to be 0.993, critically damped. This can be used to find the damping constant using the following equation:

$$\zeta = \frac{c}{c_c} \qquad \Rightarrow \qquad c = \zeta * c_c \tag{6}$$

where the critical damping constant coefficient is a product of the equivalent spring constant and equivalent mass as shown:

$$c_c = 2\sqrt{km} = 2\sqrt{k_{eq}m_{eq}} \tag{7}$$

Therefore, the damping constant was found to be $91.9N - s/m$. Like the spring coefficients, this is equivalent to $c_1 = c_2 = 184N - s/m$.

Mass Equivalence

Mass equivalence sees that actuator mass and platform mass would move non-synchronously due to their two degrees of freedom. This system sees both degrees as being on the same axis separated by identical springs and dampers. Mass equivalence is dependent on the displacement difference between the two masses in relation to ground. δ_{m_2} being two times δ_{m_1}. The solution for mass equivalence is shown below, where platform mass is used as the origin.

$$\frac{1}{2}m_{eq}\dot{x}^2 = \frac{1}{2}m_1\dot{x_1}^2 + \frac{1}{2}m_2\dot{x_2}^2 \tag{8}$$

The relationship between $\dot{x_1}$ & $\dot{x_2}$ is:

$$\dot{x}_1 = \dot{x_2}\frac{\delta_{m_1}}{\delta_{m_2}} = \frac{1}{2}\dot{x} \tag{9}$$

Insert (9) into (8) and simplify:

$$\frac{1}{2}m_{eq}\dot{x_2}^2 = \frac{1}{2}m_1\left(\dot{x_2}\frac{\delta_{m_1}}{\delta_{m_2}}\right)^2 + \frac{1}{2}m_2\dot{x_2}^2 \quad \Rightarrow \quad \frac{1}{2}m_{eq}\dot{x_2}^2 = \frac{1}{2}m_1\dot{x_2}^2\left(\frac{\dot{\delta_{m_1}}}{\delta_{m_2}}\right)^2 + \frac{1}{2}m_2\dot{x_2}^2 \tag{10}$$

The mass equivalence can thus be found as:

$$m_{eq} = m_1\left(\frac{\delta_{m_1}}{\delta_{m_2}}\right)^2 + m_2 = m_1\left(\frac{1}{2}\right)^2 + m_2 = \frac{m_1}{4} + m_2 \tag{11}$$

The mass of the spring has been ignored in the solution and would continue to be ignored given that it is a strip of 1mm thick 1095 steel[3], lighter than the actuator/ platform, and is attached to ground on one side. The mass of the actuator (m_1) is 42.0 ± 6.6 g[6] and the platform (m_2), as currently designed, is estimated to have a mass of 9.658g if Aluminum 6061 is used. This results in an equivalent mass of $m_{eq} = 20.15 \pm 1.64$g.

Reduction to a Single-degree-of-freedom:

Using the equivalencies found, the equation of motion was reduced to:

$$(m_1/4 + m_2)\ddot{x} + \frac{c}{2}\dot{x} + \frac{k}{2}x = F_{actuator} \tag{12}$$

Equations of Motion - System with Finger – Three-DOF

The equation of motion for the system was found using the three-DOF system, shown in Figure 9. In this context, x_1 was the displacement of the spring to the left of mass m, x_2 was the displacement of the spring to the right of mass m. This was, arguably, an unnecessary distinction given that $x_1 = x_2$ if the system performed as designed. In the third degree of freedom, the finger was assumed to be free to move. While it is possible that a user might

[3] Estimated to have a mass of $2.185g$. The mass-tolerance on the actuator exceeds the mass of the spring.

impose a vibration load on the system, it was assumed that the user's finger would remain static, and the actuator would supply all oscillating load.

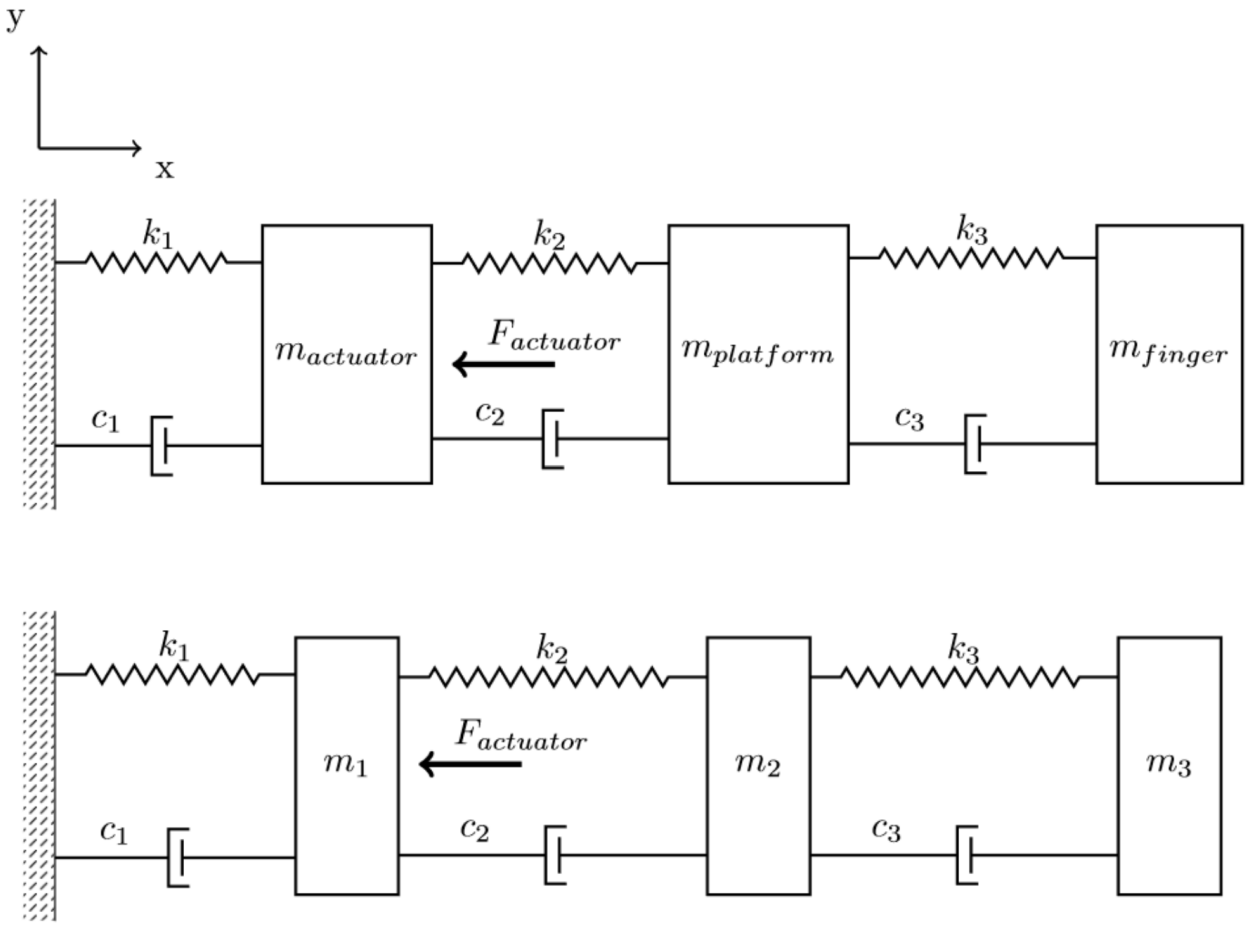

Figure 9: The Built-Out System for Actuator 1, the Top Being the Labeled Masses, the Bottom Being their Numbered Equivalents.

Sum of the Forces for the Actuator, Mass 'm_1'

$$\Sigma F - m\ddot{x}_1 = 0 \quad \Rightarrow \quad -m_1\ddot{x_1} = -F_{actuator} + k_1x_1 + c_1\dot{x}_1 + k_2(x_1 - x_2) + c_2(\dot{x}_1 - \dot{x}_2) \tag{13}$$

$$F_{actuator} = m_1\ddot{x}_1 + \dot{x}_1(c_1 + c_2) + \dot{x}_2(-c_2) + x_1(k_1 + k_2) - k_2x_2 \tag{14}$$

Sum of the Forces for the Platform, Mass 'm_2'

$$\Sigma F = -m_2\ddot{x}_2 = \ -k_2(x_1 - x_2) + k_3(x_2 - x_3) - c_2(\dot{x}_1 - \dot{x}_2) + c_3(\dot{x}_2 - \dot{x}_3) \tag{15}$$

$$0 = m_2\ddot{x}_2 + -c_2\dot{x}_1 + \dot{x}_2(c_2 + c_3) - c_3\dot{x_3} - k_2x_1 + x_2(k_2 + k_3) - k_3x_3 \tag{16}$$

Sum of the Forces for the Platform, Mass 'm_3'

$$\Sigma F = -m_3\ddot{x_3} = \ -F_{finger} - k_3(x_2 - x_3) - c_3(\dot{x}_2 - \dot{x}_3) \tag{17}$$

$$F_{user} = m_{3\ddot{x}_3} - c_3\dot{x}_2 + c_3\dot{x}_3 - k_3x_2 + k_3x_3 \tag{18}$$

Equation of Motion for the Three-DOF System

$$\begin{bmatrix} m_1 & 0 & 0 \\ 0 & m_2 & 0 \\ 0 & 0 & m_3 \end{bmatrix} \begin{Bmatrix} \ddot{x}_1 \\ \ddot{x}_2 \\ \ddot{x}_3 \end{Bmatrix} + \begin{bmatrix} c_1 + c_2 & -c_2 & 0 \\ -c_2 & c_2 + c_3 & -c_3 \\ 0 & -c_3 & c_3 \end{bmatrix} \begin{Bmatrix} \dot{x}_1 \\ \dot{x}_2 \\ \dot{x}_3 \end{Bmatrix} + \begin{bmatrix} k_1 + k_2 & -k_2 & 0 \\ -k_2 & k_2 + k_3 & -k_3 \\ 0 & -k_3 & k_3 \end{bmatrix} \begin{Bmatrix} \mathrm{x}_1 \\ x_2 \\ \mathrm{x}_3 \end{Bmatrix} = \begin{Bmatrix} F_{actuator} \\ 0 \\ F_{finger} \end{Bmatrix} \quad (19)$$

Reduction to a Single-degree-of-freedom:

The reduction of the system with the finger closely resembled that of the reduction without the finger. All nodes are in parallel, and the motion of masses is identical. As seen in Figure 9, all nodes are parallel in the multi-degree of freedom system. In the event of a parallel system, the reduction for spring and viscous damping is:

$$c_{eq} = \frac{1}{\frac{1}{c_1}+\frac{1}{c_2}+\frac{1}{c_3}} \quad (20)$$

$$k_{eq} = \frac{1}{\frac{1}{k_1}+\frac{1}{k_2}+\frac{1}{k_3}} \quad (21)$$

The mass equivalence was found by assuming that the displacement of m_2 and m_3 would be twice that of m_1. This assumption was based on the motion of m_2 being that of $2x_1$ and m_3 was assumed to move in tandem with m_2. Given this assumption, the mass equivalence became:

$$\frac{1}{2}\mathrm{m_{eq}}\dot{\mathrm{x}}^2 = \frac{1}{2}m_1\dot{\mathrm{x}}_1^{\,2} + \frac{1}{2}m_2(\dot{\mathrm{x}}_1 + \dot{\mathrm{x}}_2)^2 + \frac{1}{2}m_3(\dot{\mathrm{x}}_1 + \dot{\mathrm{x}}_2)^2 \quad (22)$$

$$\mathrm{m_{eq}}\dot{\mathrm{x}}_1^{\,2} = m_1\dot{\mathrm{x}}_1^{\,2} + 4m_2\dot{\mathrm{x}}_1^{\,2} + 4m_3\dot{\mathrm{x}}_1^{\,2} \quad \Rightarrow \quad \mathrm{m_{eq}} = m_1/4 + m_2 + m_3 \quad (23)$$

With this reduction, the equation of motion for the single-degree-of-freedom system was:

$$(m_1/4 + m_2 + m_3)\ddot{x} + \frac{1}{\frac{1}{c_1}+\frac{1}{c_2}+\frac{1}{c_3}}\dot{\mathrm{x}} + \frac{1}{\frac{1}{k_1}+\frac{1}{k_2}+\frac{1}{k_3}}x = F_{actuator} \quad (24)$$

Given that any force from the finger would be static and could only serve to change the center of oscillation, it was not included in any of the simulations, including the multi-degree of freedom systems.

Quantification of System Parameters:

CAD models, vibration simulations within ANSYS, and previous literature[11] suggested the values found in Table 1. Based on these values, the equations of motion were quantified.

Table 1: Mechanical Properties of the Modeled System.

Node	Spring constant $k\left(\frac{kN}{m}\right)$	Damping Coefficient $c\left(\frac{Ns}{m}\right)$	Mass m
1	408	184	42 g
2	408	184	9.66 g
3	1.4	1.6	170 mg

Quantification of the System Without a Finger:

Similar to the system with a finger, the system without a finger is shown below.

$$\begin{bmatrix}0.042 & 0\\ 0 & 0.0096\end{bmatrix}\begin{Bmatrix}\ddot{x}_1\\ \ddot{x}_2\end{Bmatrix}+\begin{bmatrix}368 & -184\\ -184 & 184\end{bmatrix}\begin{Bmatrix}\dot{x}_1\\ \dot{x}_2\end{Bmatrix}+\begin{bmatrix}816 & -408\\ -408 & 408\end{bmatrix}\begin{Bmatrix}\mathrm{x}_1\\ \mathrm{x}_2\end{Bmatrix}*10^3=\begin{Bmatrix}85cos\theta\\ 0\end{Bmatrix} \quad (27)$$

The single-degree-of-freedom reduction was thus:

$$0.020\ddot{x}+91.9\dot{\mathrm{x}}+204{,}000\mathrm{x}=85cos\theta \quad (28)$$

This reduction preserved more digits of precision given that the properties of the system were more precisely known than those of a finger.

Quantification of the System with a Finger:

The following equations modeled the system in a multi-degree of freedom system and in its reduced form. $F_{actuator}$ was arbitrary, $85N$ was selected for consistency.

$$\begin{bmatrix}0.042 & 0 & 0\\ 0 & 0.0096 & 0\\ 0 & 0 & 170*10^{-6}\end{bmatrix}\begin{Bmatrix}\ddot{x}_1\\ \ddot{x}_2\\ \ddot{x}_3\end{Bmatrix}+\begin{bmatrix}368 & -184 & 0\\ -184 & 185 & -1.6\\ 0 & -1.6 & 1.6\end{bmatrix}\begin{Bmatrix}\dot{x}_1\\ \dot{x}_2\\ \dot{x}_3\end{Bmatrix}+\begin{bmatrix}816 & -408 & 0\\ -408 & 410 & -1.38\\ 0 & -1.38 & 1.38\end{bmatrix}\begin{Bmatrix}\mathrm{x}_1\\ \mathrm{x}_2\\ \mathrm{x}_3\end{Bmatrix}*10^3=\begin{Bmatrix}85cos\theta\\ 0\\ 0\end{Bmatrix} \quad (25)$$

Reduced to a single-degree-of-freedom, the equation of motion for the system with a finger became:

$$0.02\ddot{x}+1.5\dot{\mathrm{x}}+1{,}370\mathrm{x}=85cos\theta \quad (26)$$

The conversion to a single-degree-of-freedom required a loss in the precision of all terms. The high variance in the properties of the human finger precluded simulating with many decimals of precision.

Simulation:

Vibration with Finger

The addition of a finger to the system complicated its reduction to a single-degree-of-freedom system. Figure 10 suggests that a reduction does exist. Below 100hz, the nodes moved synchronously without any indication that the nodes were in any way separate. Figure 11 demonstrated that, at higher frequencies, the nodes would not necessarily displace in similar ways; however, there was no reason to suspect that the vibration mode emerging in Figure 11 prohibited a single DOF reduction.

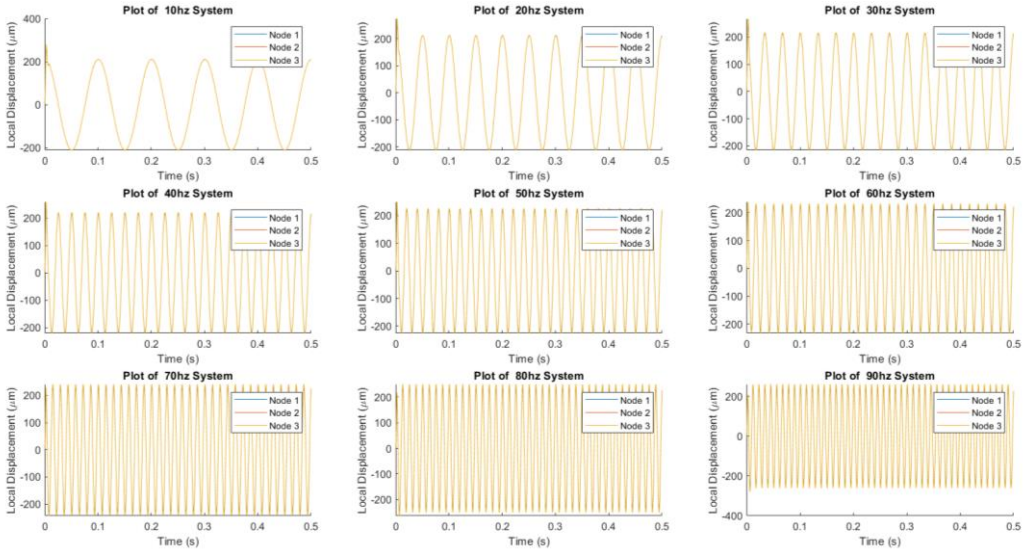

Figure 10: Plots of the Three DOF system Nodes at Low Frequencies

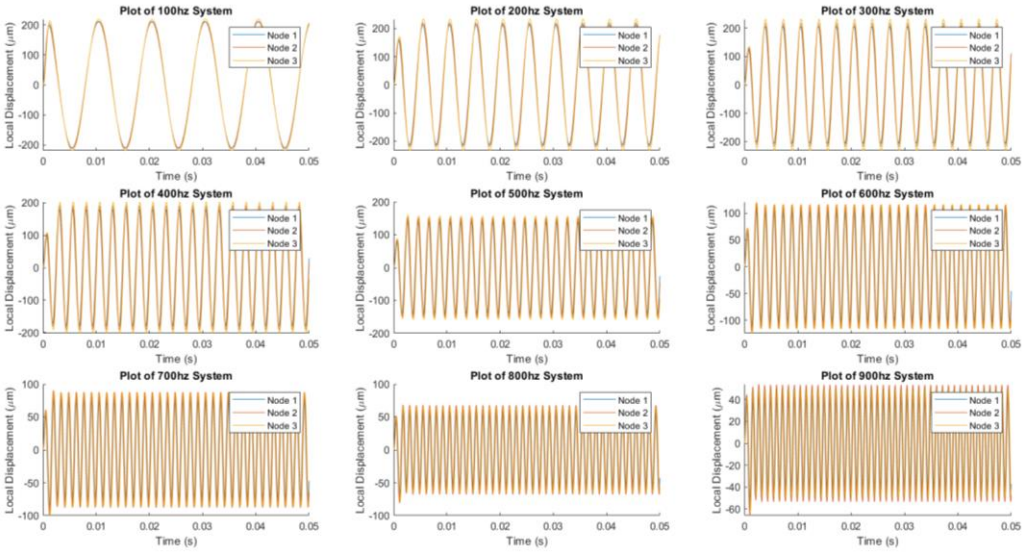

Figure 11: Plots of the Three DOF System Nodes at High Frequencies

Table 2 summarizes the behavior of both the multi DOF system and the single DOF system. As seen, the single DOF system has a low natural frequency relative to the multi DOF system. Figure 12 and Figure 13 highlight the implications of that difference in natural frequencies. The single DOF simulation exhibited beating in all plots and its vibration never resembled the stability of the multi DOF system. It was suspected that the deviations between the multi DOF and single DOF systems were driven exclusively by the introduction of the finger, as would be demonstrated below. The vibration properties of the finger have been discussed previously in Table 1. However, Figure 12 and Figure 13 suggested that the deviation of damping, mass, and spring coefficients drove the system properties outside the range that can be modeled with reduction methods. In all cases, the difference in coefficient magnitudes exceeded a factor of ten.

Table 2: Natural Frequencies for the System w. a Finger

	Natural Frequency, ω_n (Hz)
Three DOF	429
	462
	1,170
One DOF	41.2

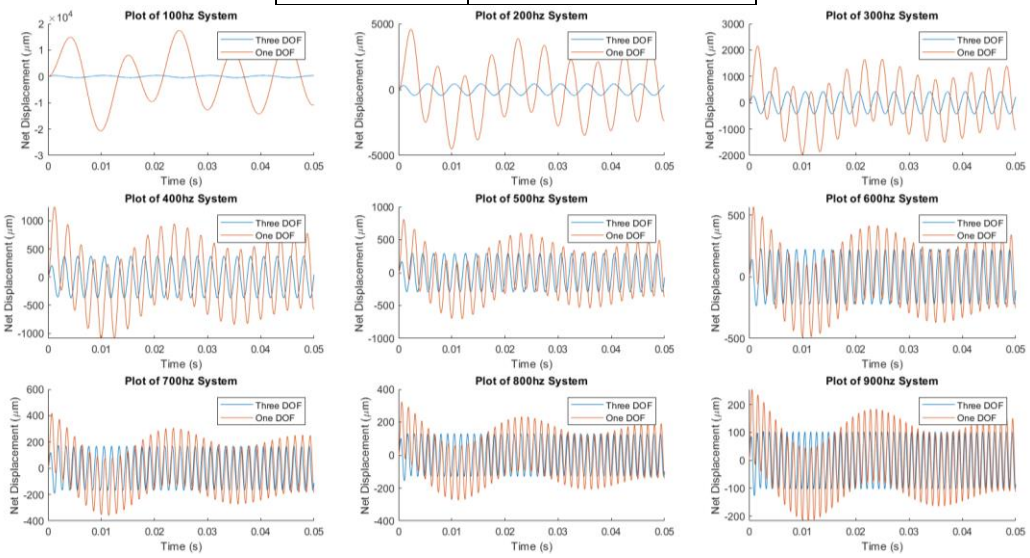

Figure 12: Plots of the Three DOF System vs. the One DOF Equivalent at High Frequencies

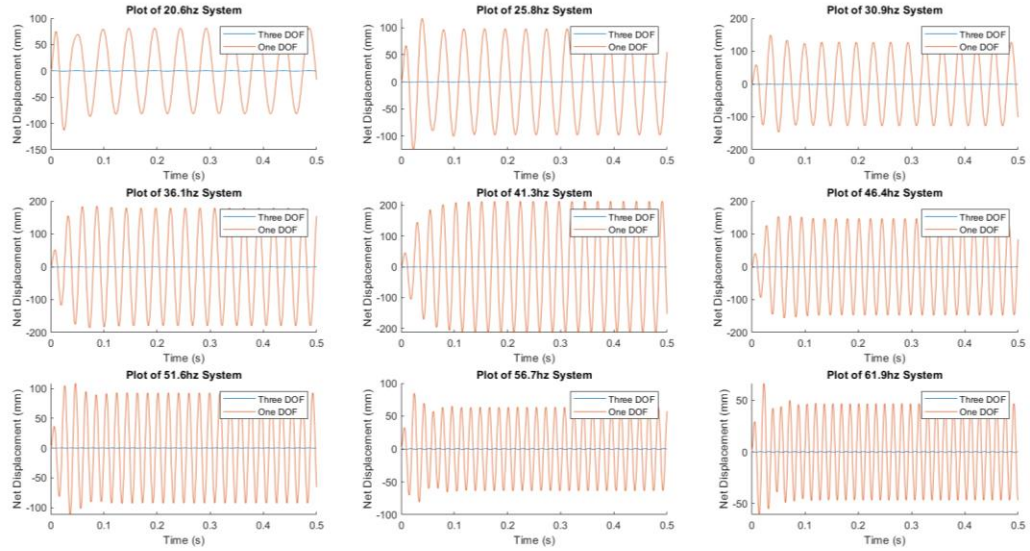

Figure 13: Plots of the Three DOF system vs. the One DOF Equivalent Near the One DOF's Resonance

Vibration without a Finger

As alluded to in the previous section, when modeled without the finger, the reduction of the system to a single-degree-of-freedom was uncomplicated. Figure 14 and Figure 15 demonstrated stable behavior across a broad range of frequencies, behavior consistent with a single-degree-of-freedom reduction. At higher frequencies, drift towards a vibration mode emerged. Despite this, the nodes remained mostly synchronous in their vibration behavior.

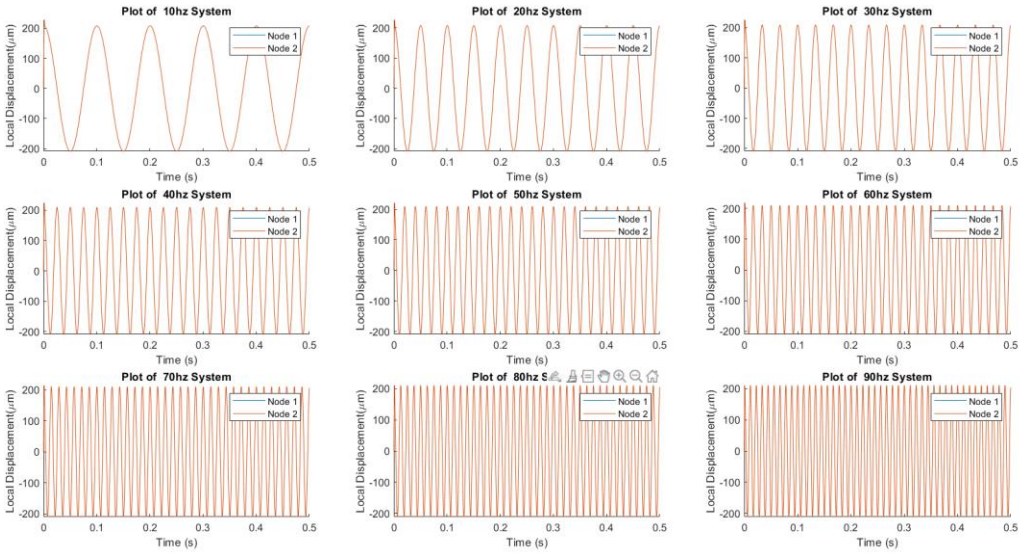

Figure 14: Plots of the Two DOF System Nodes at Low Frequencies

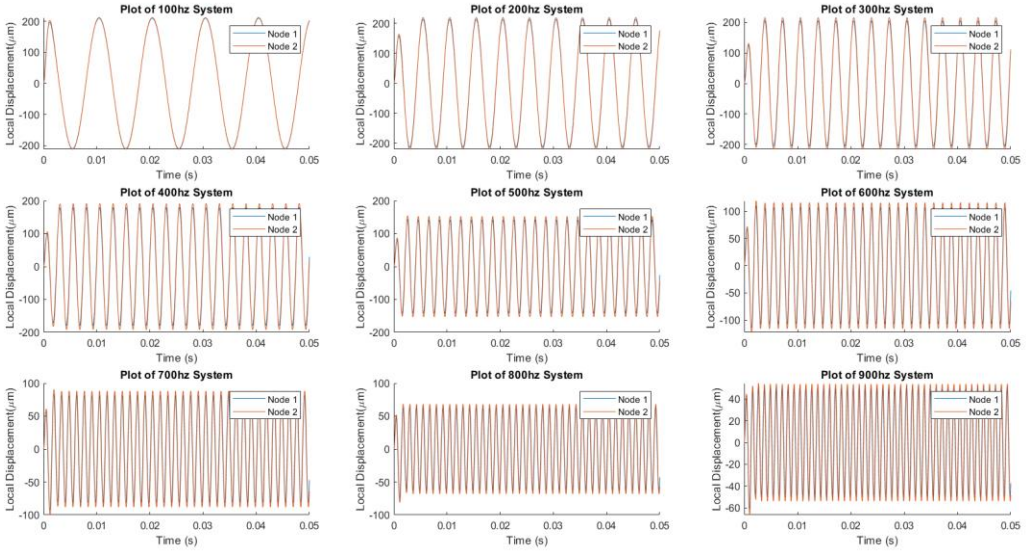

Figure 15: Plots of the Two DOF System Nodes at High Frequencies

As seen in Table 3, the one DOF reduction more closely resembled that of the system it was intended to model. If the natural frequency is any indication, the one DOF reduction may also better simulate the behavior of the system with a finger, hinting that it may not be possible to reduce the system with a finger to a single-degree-of-freedom a priori. Figure 16 and Figure 17 reinforced the perception that the single-degree-of-freedom system was a valid reduction, seeing as both systems exhibited similar behaviors across a broad span of frequencies, especially near resonance.

Table 3: Behaviors of the System without a Finger

	Natural Frequency, ω_n (Hz)
Two DOF	438
	1,171
One DOF	506

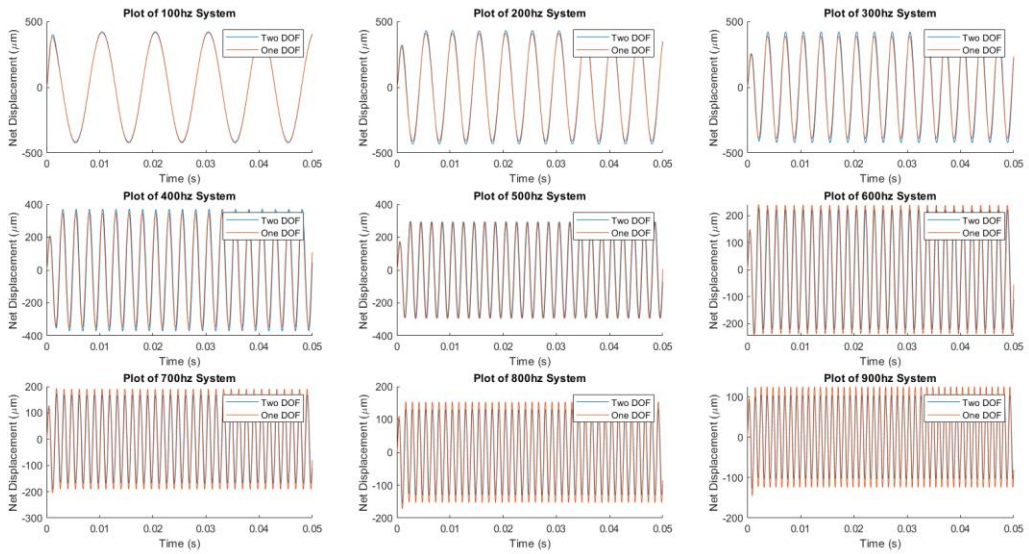

Figure 16: Plots of the Two DOF System vs. the One DOF Equivalent at High Frequencies

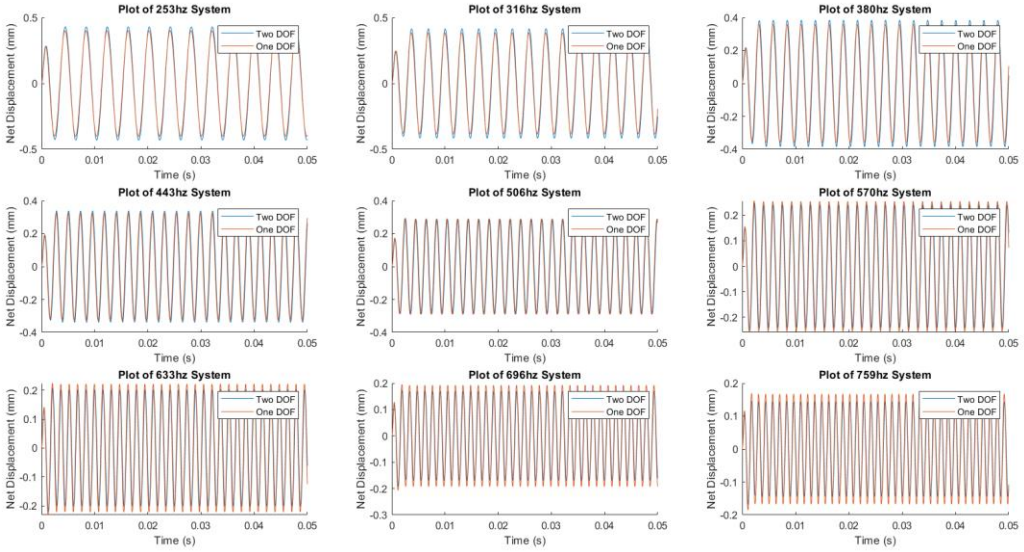

Figure 17: Plots of the Two DOF System vs. the One DOF Equivalent Near Resonance

Conclusion

The introduction of a human finger strongly influences the ability to reduce a haptic device to a single-degree-of-freedom. Simulations without a finger suggest that haptic devices resembling the flextensional actuator shown can be reduced to a single-degree-of-freedom without complication. The introduction of the finger to the simulation complicated the reduction. Traditional reduction methods result in a single-degree-of-freedom system that does not resemble its multi-degree-of-freedom equivalent. The study confirms that it is not possible to understand the frequency behavior of the actuator-finger system prior to a simulation of the multi-degree-of-freedom model.

References

[1] R. A. R. Picone, D. Webb, and B. Powell, “Metastimuli: An Introduction to PIMS Filtering,” in *Augmented Cognition. Human Cognition and Behavior*, vol. 12197, D. D. Schmorrow and C. M. Fidopiastis, Eds. Cham: Springer International Publishing, 2020, pp. 118–128. doi: 10.1007/978-3-030-50439-7_8.

[2] R. A. R. Picone, B. Powell, and J. Lentz, “Dialectical Information Architecture,” 0060417

[3] L. A. Jones, *Haptics*. Cambridge, Massachusetts: The MIT Press, 2018.

[4] T. L. Gibo, W. Mugge, and D. A. Abbink, “Trust in haptic assistance: weighting visual and haptic cues based on error history,” *Experimental Brain Research*, vol. 235, no. 8, pp. 2533–2547, Aug. 2017, doi: 10.1007/s00221-017-4986-4.

[5] G. Robles-De-La-Torre and V. Hayward, “Force can overcome object geometry in the perception of shape through active touch,” *Nature*, vol. 412, no. 6845, pp. 445–449, Jul. 2001, doi: 10.1038/35086588.

[6] “Multilayer Piezoelectric Actuators, AE Series Resin Coated.” KEMET. Accessed: Jul. 13, 2021. [Online]. Available: https://content.kemet.com/datasheets/KEM_P0101_AE.pdf

[7] M. E. Kiziroglou, B. Temelkuran, E. M. Yeatman, and G.-Z. Yang, “Micro Motion Amplification–A Review,” *IEEE Access*, vol. 8, pp. 64037–64055, 2020, doi: 10.1109/ACCESS.2020.2984606.

[8] M. Rohde, L. C. J. van Dam, and M. O. Ernst, “Statistically Optimal Multisensory Cue Integration: A Practical Tutorial,” *Multisens Res*, vol. 29, no. 4–5, pp. 279–317, 2016, doi: 10.1163/22134808-00002510.

[9] B. Sauvet, T. Laliberté, and C. Gosselin, “Design, analysis and experimental validation of an ungrounded haptic interface using a piezoelectric actuator,” *Mechatronics*, vol. 45, pp. 100–109, Aug. 2017, doi: 10.1016/j.mechatronics.2017.06.006.

[10] C.-H. Yeh *et al.*, “Application of piezoelectric actuator to simplified haptic feedback system,” *Sensors and Actuators A: Physical*, vol. 303, p. 111820, Mar. 2020, doi: 10.1016/j.sna.2019.111820.

[11] M. Wiertlewski and V. Hayward, “Mechanical behavior of the fingertip in the range of frequencies and displacements relevant to touch,” *Journal of Biomechanics*, vol. 45, no. 11, pp. 1869–1874, Jul. 2012, doi: 10.1016/j.jbiomech.2012.05.045.